scientific reports

Check for updates

OPEN

Adsorption of Cr(VI) ions from wastewater using water-based polyacrylic resin

Yunwei Huang[1,2], Shaoyu Lin[1], Pingke Ai[3], Chunsheng Li[1,2], Feihua Ye[1,2]✉, Jiaping Gan[1], Jiachun Xu[1], Lingling Su[1], Qiumin Chen[1], Junhua Chen[1,2] & Jiangfei Cao[1,2]✉

Hexavalent chromium (Cr(VI)) contamination in water poses severe environmental and health risks, necessitating efficient and sustainable removal technologies. A water-based polyacrylic resin was synthesized via inverse emulsion polymerization using methyl methacrylate, acrylic acid, and maleic anhydride, thereby avoiding the use of organic solvents. Under optimal conditions (0.8 g dosage, pH 2, 318 K, 12 h), the resin achieves 98.73% Cr(VI) removal from 1 mg/L wastewater, following the pseudo-second-order kinetic model (R^2 = 0.9927). Furthermore, the adsorption is well-fitted to the Langmuir model (R^2 = 0.9911), yielding a calculated maximum adsorption capacity of 142.86 mg/g. FTIR analysis confirms chemisorption via Cr–O bond formation as the key mechanism. Thermodynamic analysis supports this chemisorption dominance, revealing an exothermic process (ΔH = 138.47 kJ/mol) with high spontaneity (ΔG < 0). Characterization via SEM/XRD shows the resin's 3D porous structure maintains integrity post-adsorption. Significantly, acid–base elution enables high regeneration efficiency (> 93%) over 5 cycles without secondary pollution. These findings highlight the promising potential of the water-based polyacrylic resin as a macromolecular adsorbent for the efficient removal of Cr(VI) ions from wastewater, offering a viable solution for wastewater treatment.

Keywords Water-based polyacrylic resin, Heavy metal, Cr(VI) ions, Chemisorption, Removal efficiency

Hexavalent chromium (Cr(VI)) contamination in water poses severe environmental and health risks due to its persistence, toxicity, and bioaccumulation potential[1–5]. Cr(VI) is widely used in industries such as electroplating, leather tanning, and dye manufacturing, generating large volumes of hazardous wastewater[6–9]. Unlike organic pollutants, Cr(VI) does not degrade naturally and is carcinogenic even at low concentrations (> 0.1 mg/L)[10–13]. Consequently, developing safe, cost-effective, and efficient methods for Cr(VI) removal from industrial wastewater is a critical global research priority.

Current methods for Cr(VI) removal—including adsorption, ion exchange, and membrane filtration—face significant limitations. While adsorbents like metal–organic frameworks (MOFs)[14,15] and graphene-based composites[16,17] exhibit high capacities, their complex synthesis and high costs hinder industrial adoption. Conventional techniques such as chemical precipitation generate toxic sludge[18,19], whereas polymer-based adsorbents often rely on organic solvents during synthesis, contradicting green chemistry principles[20–22]. Moreover, many existing materials rely solely on electrostatic adsorption, limiting their efficiency and reusability[23–25]. Recent studies highlight a favorable balance between high efficiency, cost-effectiveness, ease of synthesis, environmental benignity, and recyclability remains a critical challenge[26,27].

Herein, we present a water-based polyacrylic resin that addresses these challenges through three key innovations (Scheme 1). Firstly, we employ a green synthesis strategy, preparing the adsorbent entirely in an aqueous medium, thereby eliminating the need for toxic organic solvents typically used in conventional acrylate polymerization[28–31]. Secondly, the resin possesses a high density of carboxyl groups (–COOH), enabling both electrostatic adsorption and chemisorption via Cr–O bond formation. This dual-mode mechanism provides performance benefits over conventional single-function adsorbents. Lastly, the resin's remarkable reusability, achieved via mild acid washing, allows for multiple cycles without performance loss, aligning with circular economy principles.

The performance of the water-based polyacrylic resin was evaluated under varying pH, concentration, and temperature conditions, providing kinetic and thermodynamic insights (including ΔH and ΔG analysis) that

[1]School of Environmental and Chemical Engineering, Zhaoqing University, Zhaoqing 526061, China. [2]Guangdong Provincial Key Laboratory of Environmental Health and Land Resource, School of Environmental and Chemical Engineering, Zhaoqing University, Zhaoqing 526061, China. [3]Guangdong Yinyang Environmental Protection New Material Co., Ltd., Foshan 528138, China. ✉email: 862609848@qq.com; 594247917@qq.com

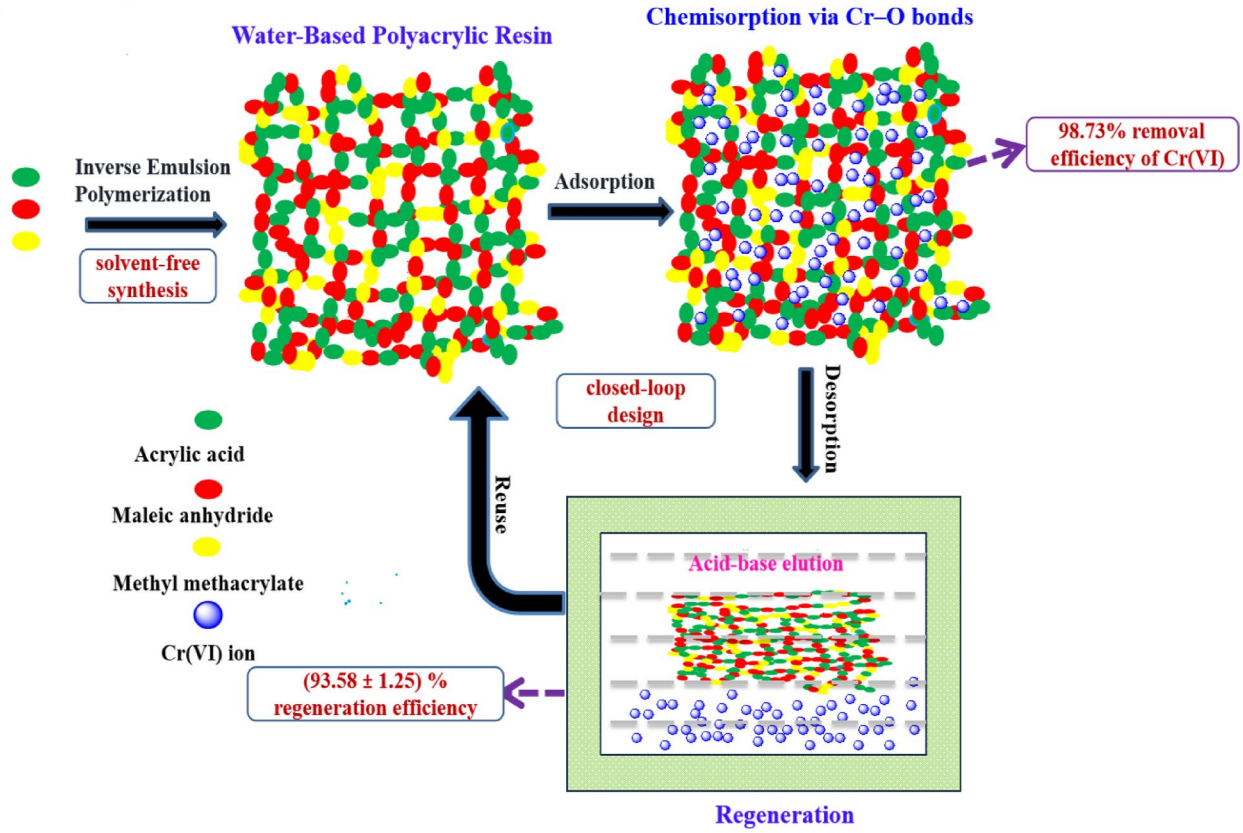

Scheme 1. Synthesis of a water-based polyacrylic resin and its application as an adsorbent for Cr(VI) Ions.

are often absent in prior adsorption Material studies[32,33]. This comprehensive characterization bridges the gap between laboratory-scale polymer design and the practical demands of industrial wastewater treatment. By offering a combination of green synthesis, high performance, and excellent recyclability, this work presents a sustainable solution aligned with the United Nations Sustainable Development Goals (SDG 6), marking an improvement over many existing adsorbents in terms of environmental footprint, efficiency, and practical applicability .

Materials and methods

Materials

Acrylic acid (CP, Chengdu Kelong Chemical Reagent Factory), Methyl methacrylate, (CP, Shanghai Jingchun Biochemical Technology Co., Ltd.), Ammonium persulphate (AR, Chengdu Kelong Chemical Reagent Factory), Maleic anhydride (AR, Hubei Zhongliao Chemical Co., Ltd.), Sodium dodecyl sulfonate (AR, Sinopharm Group Chemical reagent Co., Ltd.), Potassium dichromate (AR, Chengdu Kelon Chemical Reagent Factory), 1,5-Diphenylcarbazid (AR, Tianjin Kemiou Chemical Reagent Co., Ltd.), Phosphoric acid (AR, Tianjin Guangcheng Chemical Reagent Co., Ltd.), Acetone (AR, Guangzhou Chemical Reagent Factory), Hydrochloric acid (AR, Guangzhou Chemical Reagent Factory), Sulphuric acid (AR, Guangzhou Chemical Reagent Factory), Sodium hydroxide (AR, Guangzhou Chemical Reagent Factory).

Preparation of water-based polyacrylic resin

The water-based polyacrylic resin is synthesized using the reverse emulsion polymerization method[34], and the experimental setup is depicted in Fig. 1. Beginning with 48 mL of distilled water poured into a 250 mL round-bottomed flask, 0.7 g of Sodium dodecyl sulfonate is added. The mixture is mechanically agitated to create a complete emulsion. After the temperature reaches 60 °C, the monomers maleic anhydride (10 g), methyl methacrylate (20 mL), and acrylic acid (2 mL) are sequentially added to the flask. At the same time, 0.5 g of ammonium persulfate is added to initiate polymerization. The reaction mixture is continuously stirred until the temperature increases to 78 °C, at which point it is maintained for 2 h. After this time, stirring is stopped, and the mixture is allowed to cool for an additional 30 min.

Once the reaction is complete, ethanol is employed as a solvent for a series of centrifugal separations to purify the polymer product. The desired water-based polyacrylic resin is then obtained by vacuum-drying it at 40 °C and 35 mbar for 24 h.

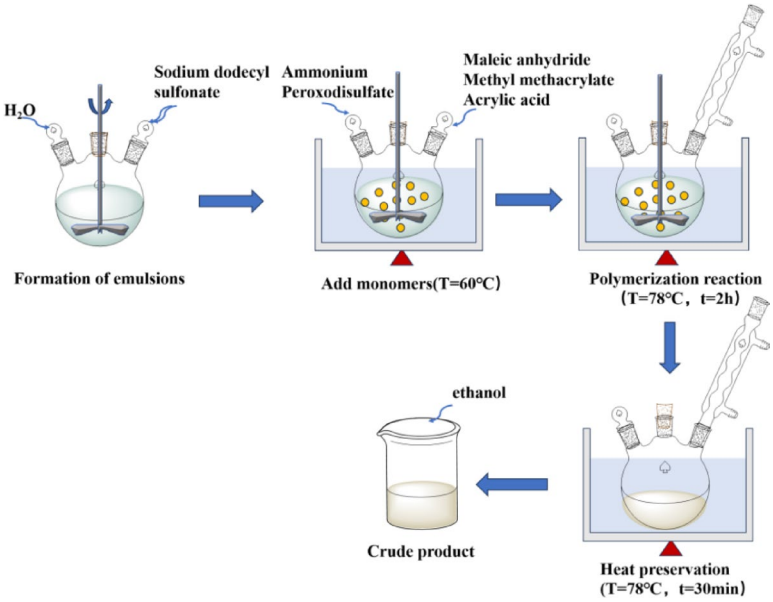

Fig. 1. Experimental set-up for preparing water-based polyacrylic resin.

Characterizations

The surface morphology and structural alterations of the water-based polyacrylic resin before and after adsorption of Cr(VI) ions were investigated using scanning electron microscopy (SEM) equipped with a Czech TESCAN MIRA LMS system. Fourier Transform Infrared (FTIR) spectroscopy was conducted on a Bruker PMA-50 spectrometer, scanning across a wavelength range of 400–4000 cm^{-1}. The thermal stability of resins was tested by thermogravimetric analysis using TG–DTA with a heating rate of 10 °C/min from 29 to 600 °C at a heating rate of 10 °C/min, under a constant nitrogen flow rate of 50 mL/min. Additionally, the crystallinity characteristics of the resin before and after the adsorption of Cr(VI) ions were investigated through X-ray diffraction (XRD) analysis.

Origin of the wastewater

To conduct this experiment, simulated wastewater samples were prepared with varying concentrations of Cr(VI) ions, using analytical-grade potassium dichromate ($K_2Cr_2O_7$) as the source of chromium.

Adsorption study

A precise amount of water-based polyacrylic resin is carefully measured and added to the wastewater solution. After optimizing the adsorption conditions, the resin is allowed to interact with the wastewater for a predetermined period. Following the adsorption phase, the remaining concentration of Cr(VI) ions in the wastewater is quantified using UV–Vis spectrophotometry. Subsequently, the removal efficiency and adsorption capacity are calculated using using Eqs. (1) and (2), respectively.

$$R\,(\%) = 100 * (C_o - C_e)/C_o \tag{1}$$

$$Q = V * (C_o - C_e)/m \tag{2}$$

Here, R and Q represent the removal efficiency and adsorption capacity (mg/g), respectively. C_o denotes the initial concentration of Cr(VI) in the wastewater before adsorption (mg/L), and C_e refers to the equilibrium concentration of Cr(VI) in the wastewater after adsorption (mg/L). V (L) is the volume of wastewater, and m (g) is the mass of water-based polyacrylic resin.

Quantitative analysis of Cr(VI)concentration in wastewater

Spectrophotometric analysis is employed to quantify Cr(VI) ions in wastewater samples using diphenylcarbazide (DPCI) as a color-developing reagent. In an acidic medium, Cr(VI) reacts with DPCI to form a distinct purple-red complex. The absorbance of this complex, measured at its maximum wavelength of 540 nm using a spectrophotometer, is then determined. The procedure begins by pipetting 5 mL of the wastewater sample into a colorimetric cuvette. Subsequently, 1 mL of a mixed acid solution (equal parts sulfuric and phosphoric acid) is added, followed by 2 mL of the DPCI solution. The mixture is then diluted to the mark with distilled water. To account for background interference, the measured absorbance is corrected by subtracting the value obtained from a blank control. Finally, the Cr(VI) concentration is determined by referencing the corrected absorbance against a pre-constructed calibration curve.

Results and discussion

Synthesis and characterization of the water-based polyacrylic resin

A water-based polyacrylic resin was synthesized via inverse emulsion polymerization using methacrylic ester, acrylic acid, and maleic anhydride as primary monomers. Sodium dodecyl sulfonate acted as the emulsifier, and ammonium persulfate initiated the polymerization. This resin proved effective for adsorbing Cr(VI) ions from wastewater by electrostatic adsorption and chemisorption via Cr–O bond formation. The synthetic route and adsorption mechanism are depicted in Fig. 2. To characterize the resin and the Cr(VI)-loaded product, we employed FTIR spectroscopy (Fig. 3a) and XRD (Fig. 3b) to study chemical structural changes, SEM imaging (Fig. 3c) to analyze surface morphology, and TG analysis (Fig. 3d) to evaluate thermal stability.

Figure 3a presents the FTIR spectra of the water-based polyacrylic resin before and after Cr(VI) adsorption. The spectrum of the resin shows a broad absorption band at 3444 cm^{-1}, attributed to O–H stretching vibrations. Peaks at 1701 cm^{-1} and 1161 cm^{-1} correspond to the C=O and C–O stretching vibrations of carboxyl groups, respectively. The absence of the C=C monomer peak (1640 cm^{-1}) confirms complete polymerization, consistent with findings in acrylic resin studies[35]. After Cr(VI) adsorption, shifts are observed: the O–H stretching peak shifts to 3535 cm^{-1}, while the C=O and C–O peaks shift to 1720 cm^{-1} and 1146 cm^{-1}, respectively, indicating coordination between chromium ions and the water-based polyacrylic resin[36,37]. Additionally, peaks appearing in the 750–975 cm range are attributed to Cr–O bands formed after Cr(VI) adsorption[38,39].

The amorphous nature of the resin, confirmed by XRD (Fig. 3b) showing broad peaks near 9° and 20° for both the pristine and Cr(VI)-loaded resins, further supports this interaction model. The peak positions and shapes remain largely unchanged, indicating the resin's amorphous structure is preserved upon Cr(VI) adsorption. Potentially hindering crystallization, a minor reduction in peak intensities at 14° and 28° after adsorption might suggest the formation of a three-dimensional network complex with chromium ions.

SEM images (Fig. 3c) reveal the morphology of the resin before and after Cr(VI) adsorption. The resin exhibits an intricate, porous network of roughly circular pores with varying diameters, nested within each other to form a rugged three-dimensional structure. This architecture provides abundant active sites and diffusion channels, enhancing adsorption capacity and kinetics. After Cr(VI) adsorption, while the basic pore structure is retained, rounded protrusions indicating partial pore blockage are visible. This blockage is likely due to the formation of insoluble chromium deposits during adsorption. Nevertheless, the overall structural integrity of the resin is maintained, which is advantageous for potential reuse and recycling.

Thermogravimetric analysis (Fig. 3d) assessed the thermal stability of the resin and the Cr(VI)-loaded resin from 29 to 600 °C. Both resins exhibit two primary weight loss stages, suggesting that Cr(VI) adsorption does not significantly compromise thermal stability. For the resin, the initial loss (29–250 °C) corresponds to

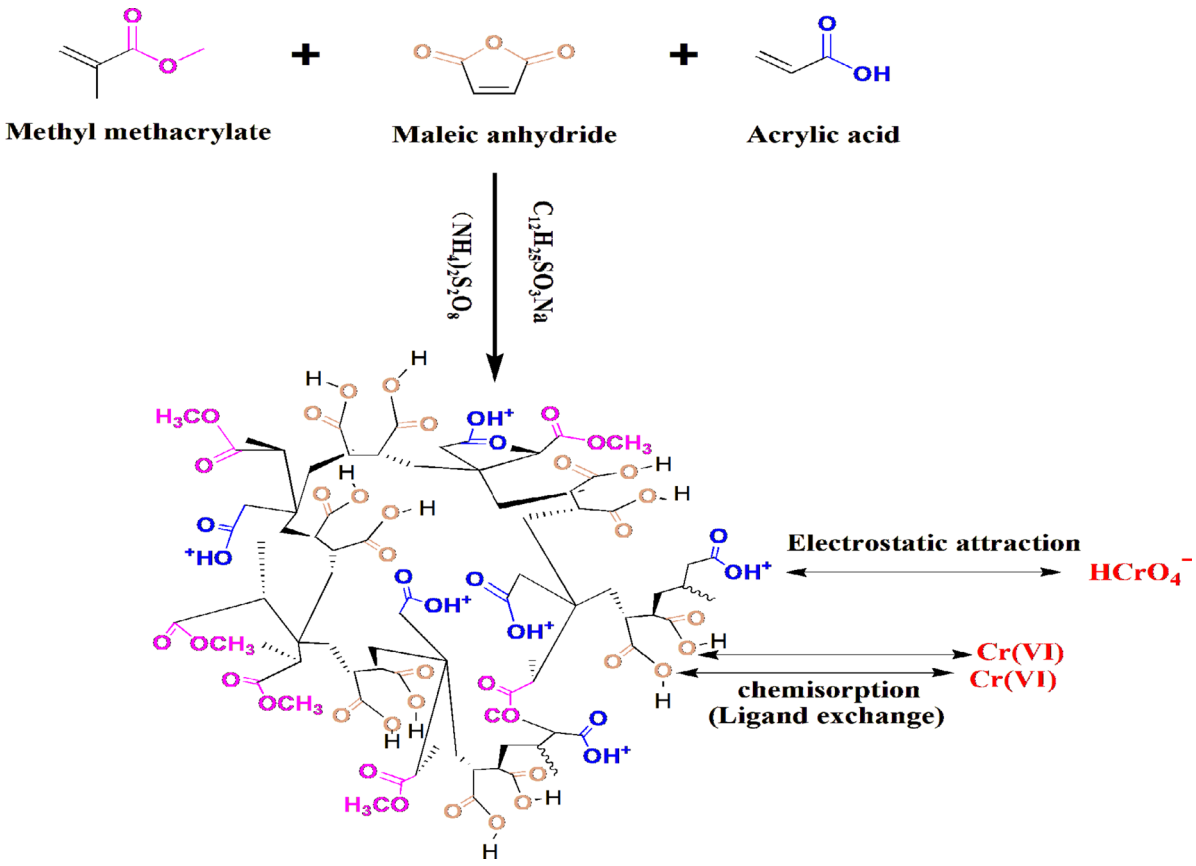

Fig. 2. Synthetic route and adsorption mechanism of the water-based polyacrylic resin.

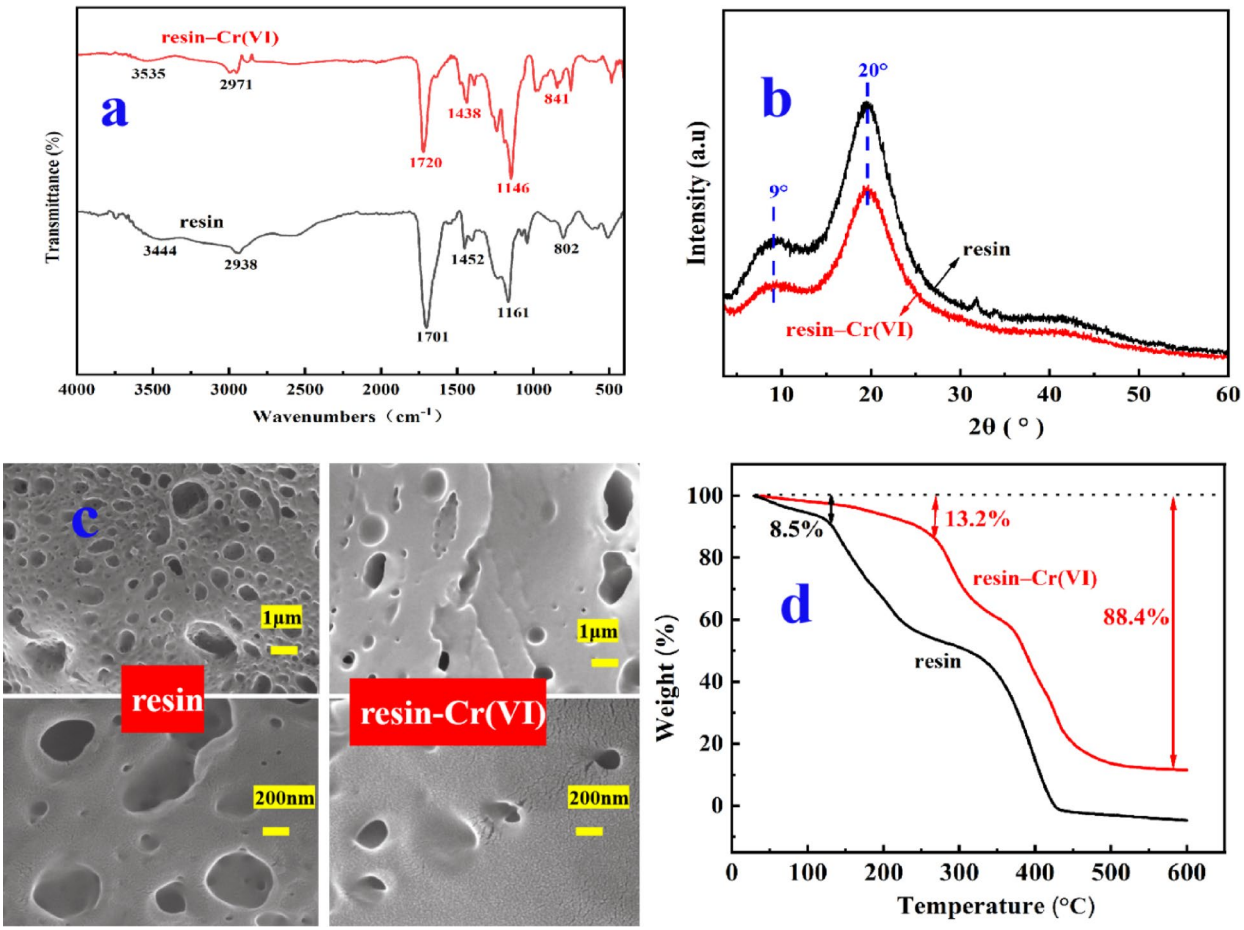

Fig. 3. FT-IR spectra (**a**), XRD spectra (**b**), SEM micrograph (**c**) and TG diagram (**d**) of the water-based polyacrylic resin and water-based polyacrylic resin–Cr(VI).

adsorbed water evaporation, followed by carboxyl group decomposition (250–430 °C). The Cr(VI)-loaded resin shows similar stages, occurring slightly at higher temperatures (29–300 °C) for water loss, 300–500 °C for decomposition. The water loss rate increases from 8.5 to 13.2% upon Cr(VI) adsorption, with the temperature range for this loss extending. The final residue content of 11.6% is attributed to chromium oxide, confirming effective Cr(VI) uptake by the resin.

Effect of the pH and initial Cr(VI) concentration (Co) on adsorption

The influence of pH on the adsorption efficiency of Cr(VI) onto the water-based polyacrylic resin is presented in Fig. 4a. The experiments were conducted under standardized conditions: a constant resin dosage of 0.8 g, an initial Cr(VI) concentration of 1 mg/L, a temperature of 318 K, and an adsorption duration of 12 h. A clear correlation between pH and removal efficiency was observed, with optimal performance achieved at pH 2, yielding a maximum removal efficiency of 98.73%. This indicates that acidic conditions strongly favor the adsorption process[40]. Removal efficiency progressively decreased as the pH increased beyond the optimal point. This decline is primarily attributed to increased competition from hydroxide ions (OH^-) for limited active adsorption sites on the resin surface. Furthermore, under alkaline conditions, Cr(VI) may hydrolyze, form less adsorbable species, or precipitate as chromium hydroxides, further diminishing the resin's efficiency. Therefore, the optimal pH for maximizing Cr(VI) removal by this resin is approximately 2. This finding aligns with the general behavior of many Cr(VI) adsorbents, where low pH promotes positively charged surface sites and the presence of highly adsorbable Cr(VI) species (e.g., $HCrO_4^-$ or $Cr_2O_7^{2-}$ under acidic conditions), facilitating electrostatic attraction and potential complexation mechanisms.

Figure 4b illustrates the relationship between the removal efficiency of Cr(VI) and its initial concentration (Co) in the wastewater, maintained at pH 2, using a resin dosage of 0.8 g, an adsorption time of 12 h, and a temperature of 318 K. The data reveal an inverse relationship: as the initial Cr(VI) concentration increases, the percentage removal efficiency decreases. This trend occurs because the fixed amount of resin possesses a finite number of active adsorption sites and a limited maximum adsorption capacity. While the absolute amount of Cr(VI) adsorbed increases with higher initial concentrations (confirmed by adsorption isotherm studies below), the proportional removal decreases because the demand for adsorption sites outpaces the supply. This behavior is typical for adsorption processes where the adsorbent quantity is constant.

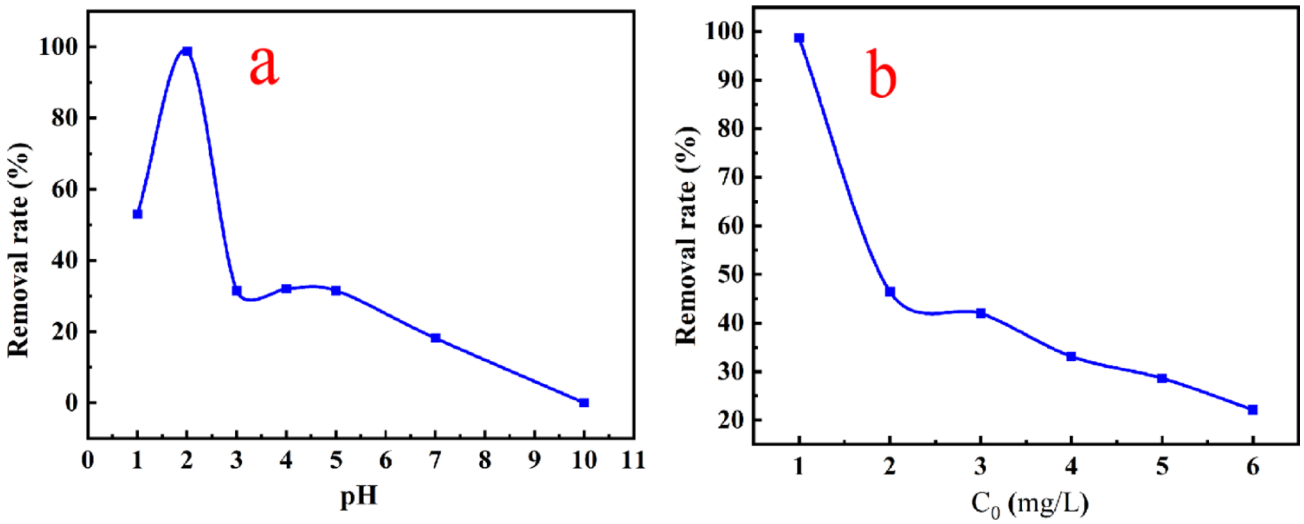

Fig. 4. Effect of the pH (**a**) and C_o (**b**) of wastewater on adsorption.

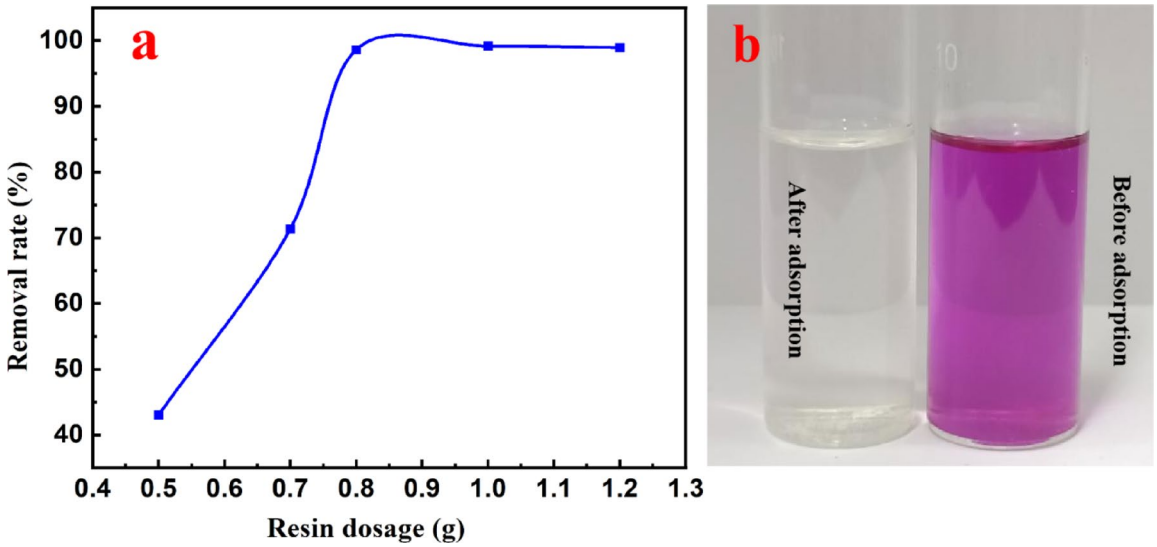

Fig. 5. Effect of the resin dosage on adsorption (**a**) and adsorption efficacy (**b**).

Effect of the resin dosage on adsorption

Figure 5 illustrates the correlation between the removal efficiency of Cr(VI) ions and the resin dosage. The experiments were conducted at a Cr(VI) concentration of 1 mg/L, pH 2, an adsorption period of 12 h, and a temperature of 318 K. The results show that the removal efficiency initially increases with increasing resin dosage, then plateaus (Fig. 5a). This is because a higher resin dose provides a larger surface area for adsorption, thereby enhancing the removal efficiency[41]. The maximum removal efficiency is achieved at a resin dosage of 0.8 g, as depicted in Fig. 5b. Beyond this optimal dosage, further increases in resin amount do not lead to a significant improvement in removal efficiency. This is attributed to the resin becoming saturated as more Cr(VI) solution passes through, reaching a point where it can no longer adsorb additional Cr(VI)[42]. Consequently, the optimal resin dosage is identified as 0.8 g.

Effect of temperature on adsorption and adsorption thermodynamics

The influence of temperature on the adsorption efficiency of Cr(VI) by the resin is shown in Fig. 6. The study was conducted with an initial Cr(VI) concentration of 1 mg/L, pH 2, a resin dosage of 0.8 g, and an adsorption duration of 12 h, varying the temperature.

As depicted in Fig. 6, the removal efficiency increases with temperature, reaching a peak of 98.73% at 318 K. Interestingly, a decline in efficiency is observed at temperatures exceeding 318 K. This temperature-dependent behavior suggests that the adsorption process is endothermic over the studied range, meaning that higher temperatures provide the necessary energy to facilitate the adsorption process. However, the observed decrease

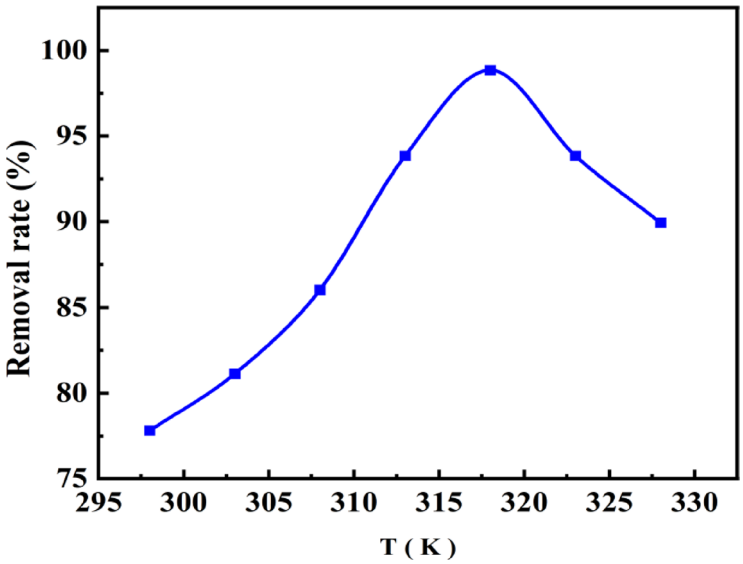

Fig. 6. Effect of temperature on adsorption.

at very high temperatures might indicate that excessive thermal energy could promote desorption of previously adsorbed Cr(VI) ions.

To further characterize the thermodynamics of the adsorption process, it is necessary to analyze the thermodynamic parameters such as the enthalpy change (ΔH), entropy change (ΔS), and Gibbs free energy change (ΔG) using Eqs. (3)–(5). Thermodynamic analysis provides critical insights into the feasibility, spontaneity, and nature (physical vs. chemical) of the adsorption process.

$$K_{\mathrm{d}} = Q_{\mathrm{e}}/C_{\mathrm{e}} \qquad (\mathrm{Kd} = \mathrm{Qe} / \mathrm{Ce3})$$

$$\ln\ K_{\mathrm{d}} = -\frac{\Delta H}{RT} + \frac{\Delta S}{R} \tag{4}$$

$$\triangle\ G = -\mathrm{RT}\ \ln K_{\mathrm{d}} \tag{5}$$

The distribution coefficient, K_{d} (L/g), quantifies the adsorption equilibrium at a given temperature (T) via Eq. (3), using the equilibrium adsorption capacity (Q_{e}, mg/g) and equilibrium concentration (C_{e}, mg/L). Enthalpy change (ΔH) and entropy change (ΔS) are determined by plotting lnKd against the inverse temperature (1/T, where T is in Kelvin, K). Utilizing the universal gas constant ($R = 8.3145$ J mol^{-1} K^{-1}), the slope and intercept of the linear regression yield ΔH and ΔS, respectively (Fig. 7). A comprehensive summary of the derived thermodynamic parameters is provided in Table 1.

The positive ΔH value, calculated to be 138.47 kJ/mol, falls within the range typically associated with chemical adsorption (20–400 kJ/mol), strongly suggesting that the interaction between Cr(VI) and the polyacrylic resin involves chemical bonding, such as complexation or ion exchange, rather than merely physical van der Waals or electrostatic forces. The positive ΔS value indicates an increase in disorder or randomness at the solid–liquid interface during adsorption. This increase can be attributed to two main factors: while Cr(VI) ions, particularly in their hydrated forms, become more ordered upon adsorption onto the resin surface, the desorption of previously bound water molecules from the adsorbent sites significantly contributes to the overall rise in entropy[43]. Such thermodynamic profiles are commonly observed in chemisorption processes involving ion exchange or complexation, where the liberation of structured water molecules plays a key role. The negative ΔG values observed at and above 318 K confirm the spontaneity and feasibility of the adsorption process within this temperature range, in accordance with the second law of thermodynamics. The increasingly negative ΔG with rising temperature further underscores the enhanced spontaneity of the adsorption at higher temperatures.

Effect of time on adsorption and adsorption kinetics

The adsorption kinetics of Cr(VI) onto the water-based polyacrylic resin were investigated under conditions of 1 mg/L initial Cr(VI) concentration, pH 2, 0.8 g resin dosage, and 318 K, as illustrated in Fig. 8. The removal efficiency was found to increase progressively with adsorption time, reaching a maximum of 98.46% after 12 h. Beyond this duration, extending the contact time did not result in a significant further increase in removal efficiency, indicating that the adsorption process had reached equilibrium. The initial rapid increase in removal efficiency suggests that accessible surface sites are quickly occupied by Cr(VI) ions[44]. The subsequent slower rate until equilibrium reflects the diffusion of Cr(VI) ions into the internal pores of the resin particles or onto less accessible sites. The plateau observed after 12 h confirms that the resin's adsorption sites have become saturated under these conditions. Therefore, an adsorption time of 12 h is determined to be sufficient for achieving near-complete removal.

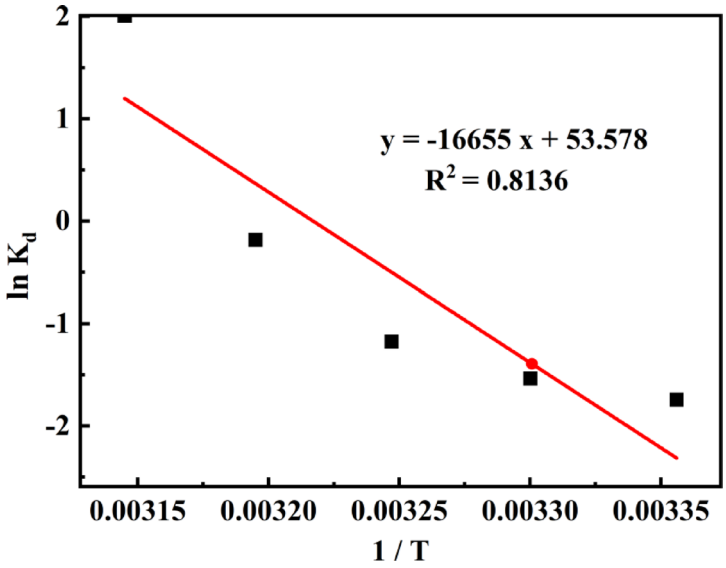

Fig. 7. The plots of ln K_d versus 1/T.

T (K)	△*G* (kJ/mol)	Δ*H* (kJ/mol)	Δ*S* (J/(mol K)
298	4.318	138.470	445.447
303	3.873		
308	3.006		
313	0.476		
318	− 5.314		

Table 1. Thermodynamic parameters.

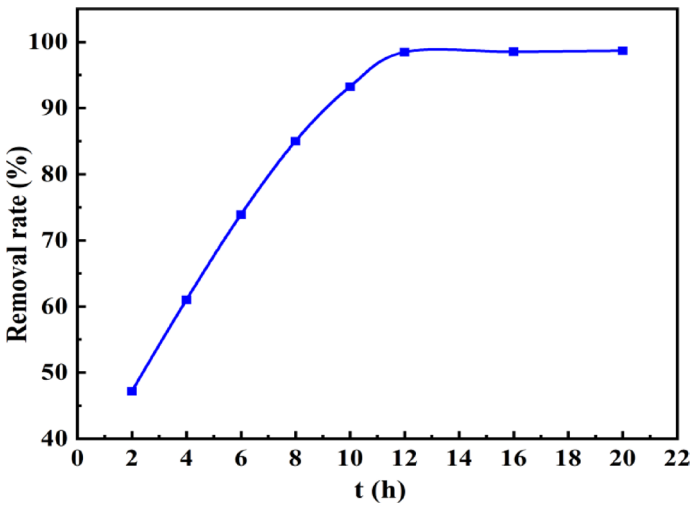

Fig. 8. Effect of time on adsorption.

To elucidate the rate-controlling mechanism of the adsorption process, kinetic data were fitted to pseudo-first-order and pseudo-second-order models (Eqs. （6） and （7）, Fig. （9a,b). Kinetic modeling is essential for understanding how quickly the adsorption process occurs and identifying the dominant mechanism, whether it be surface adsorption, intra-particle diffusion, or film diffusion. The pseudo-first-order model assumes that the rate is proportional to the difference between the equilibrium adsorption capacity (Q_e) and the adsorption capacity at time t (Q_t). The pseudo-second-order model, proposed by Ho and McKay[45], assumes that the rate is

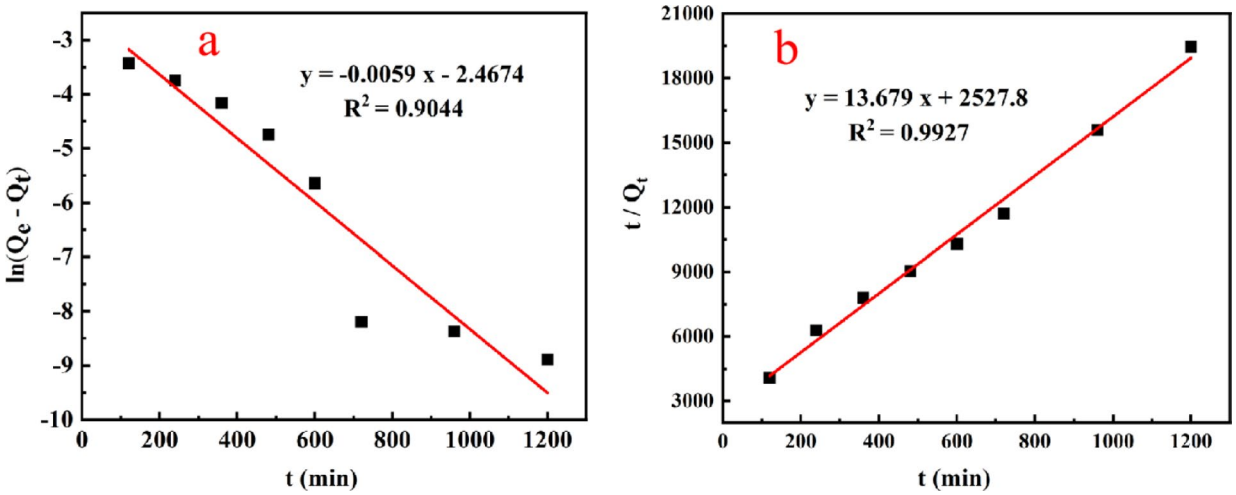

Fig. 9. quasi-first-order (**a**) and quasi-second-order (**b**) reaction.

Kinetic equation	Parameter	Value	R^2
Quasi-first-order	Q_e (mg/g)	0.0848	0.9044
	K_1 (1/min)	0.0059	
Quasi-second-order	Q_e (mg/g)	0.0731	0.9927
	K_2 (1/min)	0.0740	
	$K_2Q_e^2$ (mg/(mgmin))	3.954×10^{-4}	

Table 2. Kinetic parameters.

proportional to the square of the amount of adsorbate remaining in the solution, suggesting chemisorption as the rate-limiting step.

$$\ln\left(Q_e - Q_t\right) = \ln Q_e - K_1 t \tag{6}$$

$$t/Q_t = 1/\left(K_2 * Q_e^2\right) + t/Q_e \tag{7}$$

Here, K_1 is the pseudo-first-order rate constant (1/min), while K_2 is the pseudo-second-order rate constant (L/mg min), and $K_2Q_e^2$ represents the initial adsorption rate (mg/g min).

The kinetic parameters calculated from the data in Fig. 9 using Eqs. (6) and (7) are presented in the Table 2.

As shown in Table 2, the pseudo-second-order model provided a significantly better fit to the experimental data, evidenced by a much higher correlation coefficient ($R^2 > 0.99$) compared to the pseudo-first-order model. Furthermore, the equilibrium adsorption capacity (Q_e) calculated using the pseudo-second-order model aligns more closely with experimental observations than that derived from the pseudo-first-order model. These findings suggest that the pseudo-second-order model provides a more accurate description of Cr(VI) adsorption onto the resin, indicating that chemisorption—potentially involving electron sharing or transfer between Cr(VI) species and the resin's functional groups—is the dominant rate-limiting step in the process[46]. The relatively high values for the pseudo-second-order rate constant (K_2) and the initial adsorption rate ($K_2Q_e^2$) further corroborate the rapid kinetics of Cr(VI) uptake by this polyacrylic resin.

Competitive adsorption study

The competitive adsorption of heavy metal ions from a mixed solution was investigated using a flame-graphite atomic absorption spectrophotometer. In this study, 0.1 g of resin was employed, and the initial concentrations of the five metal ions were uniformly set at 50 mg/L. The resulting adsorption capacities for each ion are presented in Fig. 10.

As the data in Fig. 10 reveals, the resin demonstrates the highest adsorption selectivity for Cr(VI), followed by Pb(II) and Cu(II), then Zn(II), with Mn(II) showing the lowest selectivity. This selectivity can be explained as follows: Under pH 2 conditions, the adsorption of Cr(VI) by the resin occurs through both electrostatic adsorption (facilitated by protonation) and chemisorption involving Cr–O bond formation. The combined effect of these two mechanisms enhances the resin's adsorption for Cr(VI). For Pb(II) and Cu(II), their high charge density and strong complexation ability with the $-COO^-$ groups on the resin result in good adsorption selectivity. In contrast, Zn(II) has moderate affinity and its adsorption is hindered by competition from H^+ ions, affecting the resin's selectivity for it. Finally, Mn(II) is adsorbed less effectively due to its larger ionic radius and higher hydration energy.

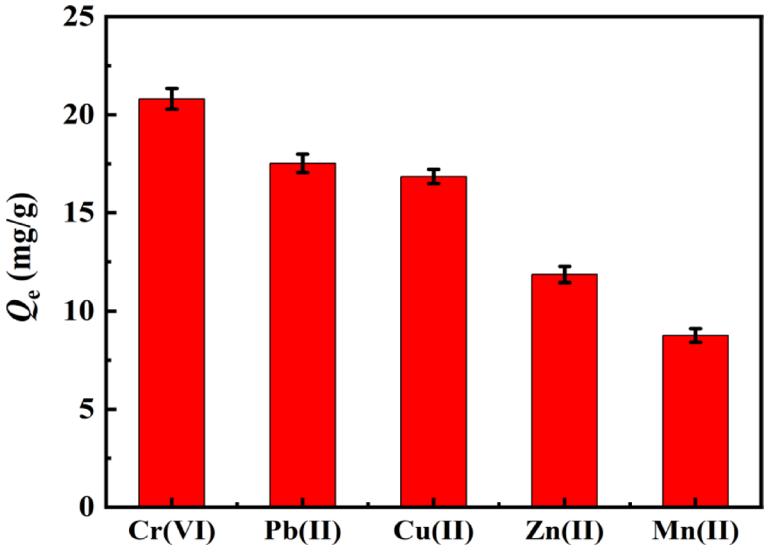

Fig. 10. Competitive adsorption of different heavy metal ions by water-based polyacrylic resin.

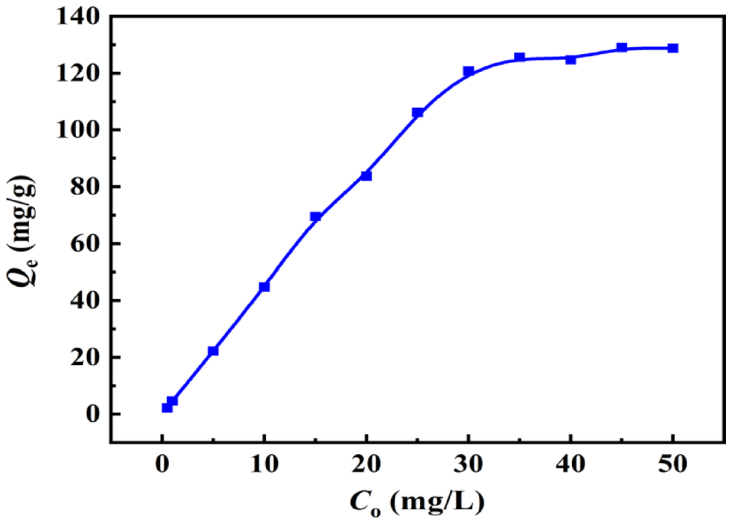

Fig. 11. Isothermal adsorption of Cr(VI) by water-based polyacrylic resin.

Isothermal adsorption study

Figure 11 illustrates the isothermal adsorption of Cr(VI) by the resin under the conditions: pH 2, resin dosage 0.01 g, and temperature 318 K. Data shows that within the initial concentration range of 0.5–30 mg/L, the adsorption capacity increases significantly with rising Cr(VI) concentration. This is attributed to the greater availability of adsorption sites on the resin at lower Cr(VI) concentrations. As the initial Cr(VI) concentration increases further, the adsorption capacity plateaus, indicating that all available adsorption sites on the resin become saturated. Consequently, increasing the Cr(VI) concentration beyond this point does not lead to additional adsorption.

To further understand the adsorption mechanism and predict the adsorption capacity under different equilibrium conditions, the experimental data were fitted to the Langmuir and Freundlich isotherm models, using Eqs. (8) and (9), respectively.

$$C_e/Q_e = C_e/Q_{max} + 1/(b * Q_{max}) \tag{8}$$

$$\ln Q_e = \ln K_f + 1/n * \ln C_e \tag{9}$$

Q_{max} (mg/g) is the theoretical maximum adsorption capacity, b (L/mg), K_f, and n are isothermal model constants. The model fitting curves for the Langmuir (shown in Fig. 12a) and Freundlich (shown in Fig. 12b) are presented below.

The model parameters calculated from the data in Fig. 12 using Eqs. (8) and (9) are presented in the Table 3.

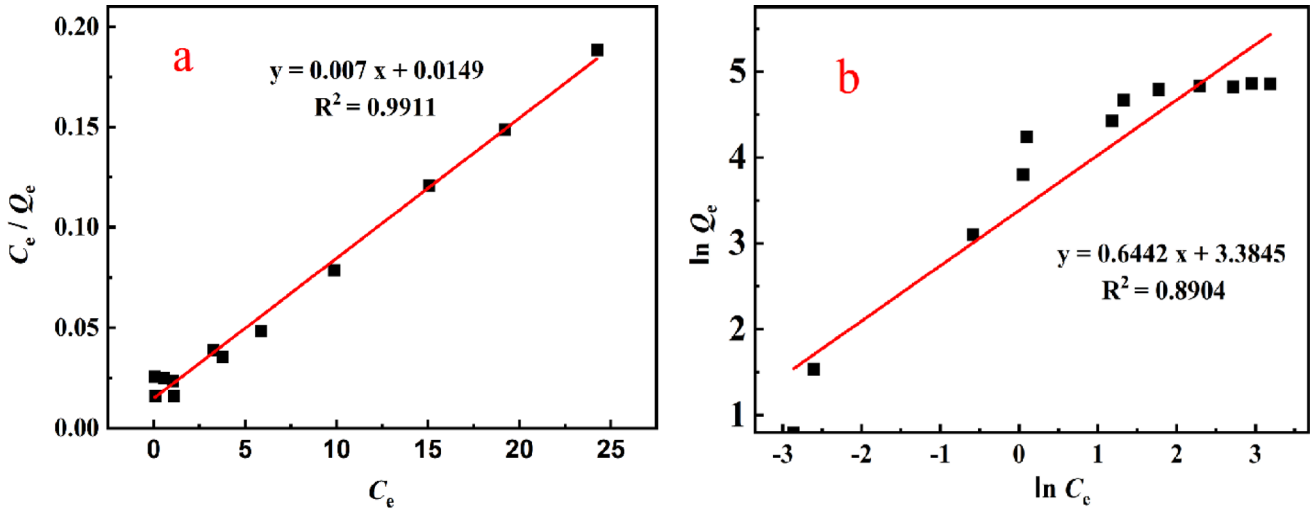

Fig. 12. Fitting curves for Langmuir (**a**) and Freundlich (**b**) models.

Model	Parameter	Value	R^2
Langmuir	Q_{max} (mg/g)	142.86	0.9911
	b (L/mg)	9.58	
Freundlich	K_f (mg/g)	29.50	0.8904
	n (1/min)	1.55	

Table 3. Parameters for isothermal adsorption of Cr(VI) by water-based polyacrylic resin.

The analysis presented in Table 3 reveals that the Langmuir model exhibits a better fit, with a correlation coefficient (R^2) of 0.9911, compared to $R^2 = 0.8904$ for the Freundlich model. The superior fit of the Langmuir model strongly suggests that the adsorption of Cr(VI) onto the water-based polyacrylic resin follows a monolayer adsorption mechanism, where Cr(VI) ions are adsorbed onto a finite number of specific active sites on the resin surface until all sites are occupied[47]. The Langmuir model also allows for the estimation of the maximum adsorption capacity (Q_m), calculated to be 142.86 mg/g. This high value underscores the considerable potential of the resin for Cr(VI) removal. Additionally, the Freundlich model, which describes multilayer adsorption on heterogeneous surfaces, was also applied. In the context of the Freundlich model, an 'n' value of 1.55, being greater than 1, generally indicates a favorable adsorption process, meaning the adsorbate has a preference for the adsorbent surface under the given conditions. This further corroborates the favorable nature of Cr(VI) adsorption onto the resin.

Regenerative capabilities of the resin

The practical applicability and economic viability of an adsorbent are significantly influenced by its recyclability. Therefore, the regeneration and reusability of the water-based polyacrylic resin for Cr(VI) adsorption were evaluated. Following adsorption, desorption was achieved using 0.2 mol/L hydrochloric acid. The resin was then collected, thoroughly rinsed with distilled water to remove residual acid and desorbed Cr(VI), soaked in a NaCl solution, and rinsed again prior to the next adsorption cycle. The results of these regeneration and reusability tests are illustrated in Fig. 13. Impressively, the resin maintained a removal efficiency of (93.58 ± 1.25) % even after five consecutive adsorption–desorption cycles. Statistical analysis (independent t-test, n = 3) confirms that the decrease in Cr(VI) removal efficiency from (97.87 ± 0.93) % in the first cycle to (93.58 ± 1.25) % in the fifth cycle is statistically significant ($p = 0.012$), demonstrating statistically significant but limited performance degradation after multiple reuses. These results highlight the regenerative capabilities of the polyacrylic resin and its potential for sustainable reuse in practical applications.

Conclusion

This study presents a novel water-based polyacrylic resin for sustainable Cr(VI) removal, featuring three key innovations. First, it utilizes an environmentally benign aqueous synthesis route, eliminating organic solvents and complex modifications. Second, it employs a dual-function mechanism combining electrostatic attraction (via –COOH groups) and chemisorption (forming Cr–O bonds, ΔH = 138.47 kJ/mol), achieving an exceptional adsorption capacity of 142.86 mg/g. Third, it incorporates a closed-loop regeneration system that maintains > 93% efficiency over 5 cycles while offering superior cost-effectiveness.

Comprehensive characterization confirms chemisorption-dominated monolayer adsorption, evidenced by pseudo-second-order kinetics ($R^2 = 0.9927$) and the Langmuir isotherm ($R^2 = 0.9911$). Thermodynamic analysis

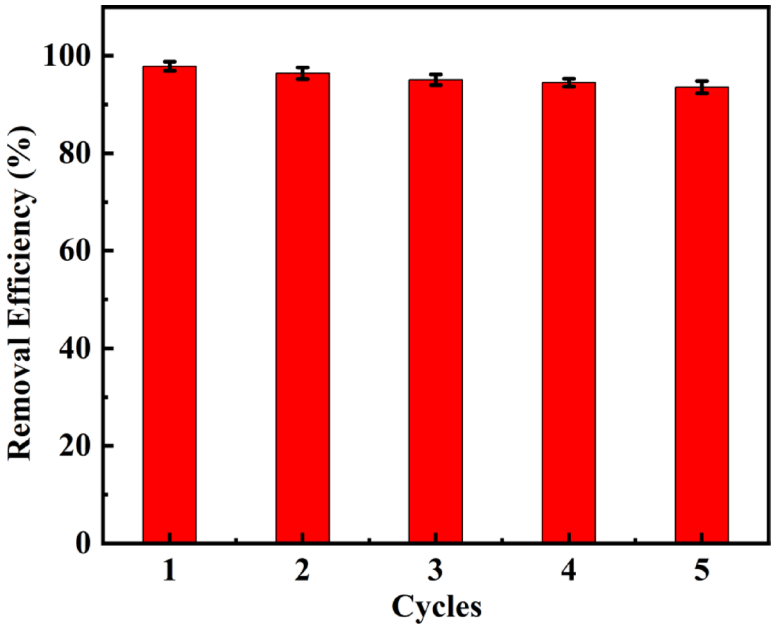

Fig. 13. Regenerative capabilities of the resin.

reveals spontaneity ($\Delta G < 0$) and an exothermic nature ($\Delta H = 138.47$ kJ/mol). Furthermore, SEM/XRD analysis confirms the remarkable structural stability of the 3D porous architecture after multiple regeneration cycles.

Compared to existing technologies, this solution addresses three critical gaps: environmental (reduced carbon footprint via solvent-free synthesis[28–31]), economic (cost advantage over graphene-based composites[16,17]), and technical (avoided the energy-intensive synthesis processes typical of MOFs[48,49]). Aligned with SDG 6 targets, this work provides an industrially scalable solution integrating green chemistry principles and circular economy viability, supported by fundamental mechanistic insights. Future research will focus on pilot-scale validation, multi-metal removal studies, and comprehensive life cycle assessments for large-scale implementation.

Data availability

The datasets used and/or analysed during the current study available from the corresponding author on reasonable request.

Received: 19 March 2025; Accepted: 9 September 2025
Published online: 13 October 2025

References

1. Mohanty, S. et al. Eco-toxicity of hexavalent chromium and its adverse impact on environment and human health in Sukinda Valley of India: A review on pollution and prevention strategies. *Environ. Chem. Ecotox.* **5**, 46–54 (2024).
2. Ramli, N. N. et al. A review of the treatment technologies for hexavalent chromium contaminated water. *Biometals* **36**, 1189–1219 (2023).
3. Igalavithana, A. D. et al. Heavy metal immobilization and microbial community abundance by vegetable waste and pine cone biochar of agricultural soils. *Chemosphere* **174**, 593–603 (2017).
4. Wan, Z. et al. Concurrent adsorption and micro-electrolysis of Cr(VI) by nanoscale zerovalent iron/biochar/Ca-alginate composite. *Environ. Pollut.* **247**, 410–420 (2019).
5. Yuan, D. et al. Removal of Cr(VI) from aqueous solutions via simultaneous reduction and adsorption by modified bimetallic MOF-derived carbon material Cu@ MIL-53 (Fe): Performance, kinetics, and mechanism. *Environ. Res.* **216**, 114616 (2023).
6. Guan, X. et al. Enhanced immobilization of chromium (VI) in soil using sulfidated zero-valent iron. *Chemosphere* **228**, 370–376 (2019).
7. Hussain, I. et al. Melamine derived nitrogen-doped carbon sheet for the efficient removal of chromium (VI). *J. Mol. Liq.* **318**, 114052 (2020).
8. Ghadikolaei, N. F. et al. Preparation of porous biomass-derived hydrothermal carbon modified with terminal amino hyperbranched polymer for prominent Cr (VI) removal from water. *Bioresour. Technol.* **288**, 121545 (2019).
9. Chakraborty, R. et al. Mechanism of chromium-induced toxicity in lungs, liver, and kidney and their ameliorative agents. *Biomed. Pharmacother.* **151**, 113119 (2022).
10. Kapoor, R. T. et al. Accumulation of chromium in plants and its repercussion in animals and humans. *Environ. Pollut.* **301**, 119044 (2022).
11. Wise, J. P. et al. Current understanding of hexavalent chromium [Cr(VI)] neurotoxicity and new perspectives. *Environ. Int.* **158**, 106877 (2022).
12. Caini, S. et al. Serum heavy metals and breast cancer risk: A case-control study nested in the Florence cohort of the EPIC (European Prospective Investigation into Cancer and nutrition) study. *Sci. Total Environ.* **861**, 160568 (2023).
13. Tumolo, M. et al. Chromium pollution in european water, sources, health risk, and remediation strategies: An overview. *Int. J. Environ. Res. Public Health* **17**(15), 5438 (2020).

14. Ahmed, K. H. et al. Synthesis of thiol functionalized MOF-808 and its efficiency for mercury removal. *Chem. Asian J.* **19**(22), e202400306 (2024).
15. Qarah, A. F. et al. Enhanced and efficient capture of Cd(II) through functionalized metal-organic frameworks embedded in a biopolymer (carboxymethyl cellulose/polyethylenimine): Thermodynamics, kinetics, and optimization via Box-Behnken methodology. *Int. J. Biol. Macromol.* **318**, 144903 (2025).
16. Guo, T. et al. Experimental and statistical physics illumination of Pb (II) adsorption on magnetic chitosan-graphene oxide surface. *Sep. Purif. Technol.* **354**, 128867 (2025).
17. Bulin, C. & Guo, T. Ultra fast and highly efficient recovery of cadmium with graphene oxide-chitosan grafted by nickel ferrite as a recyclable adsorbent and atomic scale mechanism. *Sci. Total Environ.* **991**, 179974 (2025).
18. Genua, F. et al. Geopolymer-based stabilization of heavy metals, the role of chemical agents in encapsulation and adsorption. *Polymers* **17**(5), 670 (2025).
19. Ito, A. et al. Removal of heavy metals from anaerobically digested sewage sludge by a new chemical method using ferric sulfate. *Water Res.* **34**(3), 751–758 (2000).
20. Anggraini, R. et al. New adsorbent, polymelamine crosslinked with s-trioxane for selective adsorption of precious metal. *Polymer* **33**, 128666 (2025).
21. Chaudhuri, H. et al. Polyethylenimine functionalized sulfur-containing POSS-based dendritic adsorbent for highly efficient and selective capturing of precious metal ions. *Desalination* **566**, 116925 (2023).
22. Hassan, A. & Das, N. Efficient, selective, and rapid recovery of gold from highly acidic solutions using an ionic phosphine-functionalized triptycene-based porous organic polymer. *ACS Sustain. Resour. Manag.* **2**(6), 890–897 (2025).
23. Chen, J. et al. Efficient removal of heavy metals using 1, 3, 5-benzenetricarboxylic acid-modified zirconium-based organic frameworks. *Environ. Technol. Innov.* **33**, 103516 (2024).
24. Mai, N. T. et al. Highly adsorptive removal of heavy metal, dye, and antibiotic pollutants using functionalized graphene nanosheets sono-electrochemically derived from graphitic waste. *J. Environ. Chem. Eng.* **12**(3), 113020 (2024).
25. Liu, W. et al. Ceramic supported attapulgite-graphene oxide composite membrane for efficient removal of heavy metal contamination. *J. Membr. Sci.* **591**, 117323 (2019).
26. Awual, M. R. et al. Efficient detection and adsorption of cadmium (II) ions using innovative nano-composite materials. *Chem. Eng. J.* **343**, 118–127 (2018).
27. Kubra, K. T. et al. Utilizing an alternative composite material for effective copper (II) ion capturing from wastewater. *J. Mol. Liq.* **336**, 116325 (2021).
28. Abdel-Halim, E. S. & Al-Deyab, S. S. Preparation of poly(acrylic acid)/starch hydrogel and its application for cadmium ion removal from aqueous solutions. *React. Funct. Polym.* **75**, 1–8 (2014).
29. Sarkar, A. K. et al. Efficient removal of malachite green dye using biodegradable graft copolymer derived from amylopectin and poly(acrylic acid). *Carbohydr. Carbohydr. Polym.* **111**, 108–115 (2014).
30. El-Aassar, M. R. et al. Development of azo dye immobilized poly (glycidyl methacrylate-co-methyl methacrylate) polymers composites as novel adsorbents for water treatment applications: Methylene blue-polymers composites. *Polymers* **14**(21), 4672 (2023).
31. Wawrzkiewicz, M., Wołowicz, A. & Hubicki, Z. Strongly basic anion exchange resin based on a cross-linked polyacrylate for simultaneous C.I. acid green 16, Zn(II), Cu(II), Ni(II) and phenol removal. *Molecules* **27**(7), 2096 (2022).
32. Awual, M. R. et al. Novel nanocomposite materials for efficient and selective mercury ions capturing from wastewater. *Chem Eng J* **307**, 456–465 (2017).
33. Awual, M. R. et al. Ligand based sustainable composite material for sensitive nickel (II) capturing in aqueous media. *J Environ Chem Eng* **8**(1), 103591 (2018).
34. Jiang, L. et al. Progress in synthesis and application research of poly(acrylic acid) series adsorbent resin materials. *Contemp. Chem. Ind.* **40**(8), 827–834 (2011).
35. Ma, G. Z. et al. Study on the conversion of acrylic C=C double bonds during dark reaction after UV curing using infrared spectroscopy. *Guang pu xue yu Guang pu fen xi=Guang pu* **30**(7), 1780–1784 (2010).
36. Dudev, T. & Lim, C. The effect of metal binding on the characteristic infrared band intensities of ligands of biological interest. *J. Mol. Struct.* **1009**, 83–88 (2012).
37. Markovska, L. A. et al. Investigation of the structure and properties of polyurethane compositions modified with metal-containing compounds. *Polym. J.* **42**(4), 283–291 (2020).
38. Fakhfakh, F. et al. Isotherm and kinetic modeling of Cr(VI) removal with quaternary ammonium functionalized silica. *J. Sol-Gel. Sci. Technol.* **111**(3), 921–940 (2024).
39. Stoilova, D. et al. Infrared spectroscopic study of ions included in $K_2Me(CrO_4)_2{\cdot}2H_2O$ (Me=Mg, Cd) and crystal structure of $K_2Cd(CrO_4)_2{\cdot}2H_2O$. *J. Mol. Struct.* **889**(1–3), 12–19 (2008).
40. Kubra, K. T. et al. The heavy lanthanide of Thulium (III) separation and recovery using specific ligand-based facial composite adsorbent. *Colloids Surf., A* **667**, 131415 (2023).
41. Salman, M. S. et al. Chitosan-coated cotton fiber composite for efficient toxic dye encapsulation from aqueous media. *Appl. Surf. Sci.* **622**, 157008 (2023).
42. Zare, K. et al. Enhanced removal of toxic Congo red dye using multi walled carbon nanotubes: kinetic, equilibrium studies and its comparison with other adsorbents. *J. Mol. Liq.* **212**, 266–271 (2015).
43. Pavasant, R. et al. Biosorption of Cu^{2+}, Pb^{2+}, Cd^{2+} and Zn^{2+} using dried marine green macroalga Caulerpalentillifera. *Bioresour. Technol.* **97**(18), 2321–2329 (2006).
44. Kubra, K. T. et al. Sustainable detection and capturing of cerium (III) using ligand embedded solid-state conjugate adsorbent. *J. Mol. Liq.* **338**, 116667 (2021).
45. Ho, Y. S. & McKay, G. Kinetic models for the sorption of dye from aqueous solution by wood. *Process Saf. Environ.* **76**(2), 183–191 (1998).
46. Hu, X. J. et al. Adsorption of chromium (VI) By ethylenediamine-modified cross-linked magnetic chitosan resin: Isotherms,kinetics and thermodynainics. *J. Hazard Mater.* **185**(1), 306–314 (2011).
47. Awual, M. R. et al. Green and robust adsorption and recovery of Europium (III) with a mechanism using hybrid donor conjugate materials. *Sep. Purif. Technol.* **319**, 124088 (2023).
48. Ghaedi, S. et al. Assessing the efficiency and reusability of zirconium-based MOF-biochar composite for the removal of Pb (II) and Cd (II) in single and multi-ionic systems. *J. Environ. Manage.* **380**, 125122 (2025).
49. Qian, Y. et al. Recent progress of metal-organic framework-derived composites: Synthesis and their energy conversion applications. *Nano Energy.* **111**, 108415 (2023).

Acknowledgements

This work was supported by the College Students Innovation and Entrepreneurship Training Program (No. S202410580061), the High-Level Project Training Programme of Zhaoqing University (No. GCCZK202406), the Science and Technology Innovation Guidance Project of Zhaoqing City (No. 241223110090446), and the Innovative Research Team Project of Zhaoqing University (No. TD202413).

Author contributions

.H., J.C., F.Y., and C.L. conceived and designed the experiments as well as wrote the paper. L.S., Q.C., J.G., J.X., L.S., J.C., and P.A. carried out the experiment and analyzed the data. All authors read and approved the manuscript.

Funding

The High-Level Project Training Programme of Zhaoqing University, No. GCCZK202406, the College Students Innovation and Entrepreneurship Training Program, No. S202410580061, the Innovative Research Team Project of Zhaoqing University, No. TD202413, the Science and Technology Innovation Guidance Project of Zhaoqing City, 241223110090446.

Declarations

Competing interests

The authors declare no competing interests.

Additional information

Correspondence and requests for materials should be addressed to F.Y. or J.C.

Reprints and permissions information is available at www.nature.com/reprints.

Publisher's note Springer Nature remains neutral with regard to jurisdictional claims in published maps and institutional affiliations.